Fluorescent Probes

International Edition: DOI: 10.1002/anie.201902766
German Edition: DOI: 10.1002/ange.201902766

# A Photoexcitation-Induced Twisted Intramolecular Charge Shuttle

*Weijie Chi[+], Qinglong Qiao[+], Richmond Lee, Wenjuan Liu, Yock Siong Teo, Danning Gu, Matthew John Lang, Young-Tae Chang,* Zhaochao Xu,* and Xiaogang Liu**

***Abstract:*** *Charge transfer and separation are important processes governing numerous chemical reactions. Fundamental understanding of these processes and the underlying mechanisms is critical for photochemistry. Herein, we report the discovery of a new charge-transfer and separation process, namely the twisted intramolecular charge shuttle (TICS). In TICS systems, the donor and acceptor moieties dynamically switch roles in the excited state because of an approximately 90° intramolecular rotation. TICS systems thus exhibit charge shuttling. TICSs exist in several chemical families of fluorophores (such as coumarin, BODIPY, and oxygen/carbon/silicon–rhodamine), and could be utilized to construct functional fluorescent probes (i.e., viscosity- or biomolecule-sensing probes). The discovery of the TICS process expands the current perspectives of charge-transfer processes and will inspire future applications.*

Photo-induced charge transfer and separation is a fundamental process,[1] responsible for photosynthesis,[2] and has applications in solar cells,[3] photocatalysis,[4] and fluorescence probes.[5] Greater understanding of charge-transfer and separation processes is thus important to aid in improving photochemistry. However, owing to fast photon-absorption rates and short excited state lifetime, understanding charge transfer and separation at a molecular level remains a significant challenge.

This challenge could be overcome if the model systems under study emit fluorescence (or other forms of luminescence).[1b] The changes in fluorescence output (for example, intensity, lifetime, and wavelength) provide critical information on the thermodynamics and kinetics of the charge-transfer and separation processes in the excited state, along with a plethora of other important photo-physical and -chemical information. Accordingly, studies have been conducted to investigate charge-transfer and separation mechanisms in fluorescent compounds.[6] It has been widely known that the intramolecular charge transfer (ICT) could be modulated via adjusting the "push–pull" effect in a compound consisting of an electron-donating group (EDG) and/or an electron-withdrawing group (EWG).[7] In such compounds, ICT is further enhanced upon photoexcitation. In particular, in a landmark study, Grabowski and co-workers proposed that quasi-rigid donor–acceptor (D–A) compounds could undergo approximately 90° intramolecular twisting in the excited state, greatly reinforcing charge transfer and resulting in a charge-separated state ($D^+$–$A^-$).[8] They named this mechanism twisted intramolecular charge transfer (TICT; Figure 1a). Rationalization of the TICT mechanism[9] has greatly facilitated the development of many functional materials and devices, such as bright and photostable fluorophores,[10] dark quenchers,[11] viscosity sensors,[12] and polarity sensors.[6b] Notably, charge-transfer and separation processes in both the ICT and TICT states are unidirectional, i.e., from the donor (D) to the acceptor (A) upon photoexcitation.

In this study, we report a bidirectional charge transfer process in fluorophores, whereby the roles of the donor and acceptor are dynamically reversed to allow charge shuttling after photoexcitation and approximately 90° intramolecular twisting (Figure 1a). The proposed mechanism is named twisted intramolecular charge shuttle (TICS), and we demonstrate that TICS is a general charge transfer mechanism, predicted in a broad range of fluorophores, such as coumarins, BODIPYs, and oxygen/carbon/silicon–rhodamines. We will also demonstrate that TICS enables the development of effective fluorescent probes.

We began this work by observing that **1** and **2** exhibited considerably different quantum yields ($\varphi = 92\%$ for **1** and

[*] Dr. W. Chi,[+] Dr. R. Lee, Prof. Dr. X. Liu
Science and Math Cluster,
Singapore University of Technology and Design
8 Somapah Road, Singapore 487372 (Singapore)
E-mail: xiaogang_liu@sutd.edu.sg
Dr. Q. Qiao,[+] W. Liu, Prof. Dr. Z. Xu
CAS Key Laboratory of Separation Science for Analytical Chemistry,
Dalian Institute of Chemical Physics, Chinese Academy of Sciences
457 Zhongshan Road, Dalian 116023 (China)
E-mail: zcxu@dicp.ac.cn
Y. S. Teo, D. Gu, Prof. Dr. M. J. Lang
Singapore-MIT Alliance for Research and Technology (SMART)
1 CREATE Way, Singapore 138602 (Singapore)
Prof. Dr. M. J. Lang
Department of Chemical and Biomolecular Engineering and
Department of Molecular Physiology and Biophysics,
Vanderbilt University, Nashville, TN 37235 (USA)
Prof. Dr. Y. T. Chang
Center for Self-Assembly and Complexity,
Institute for Basic Science (IBS), Pohang 37673 (Republic of Korea),
and
Department of Chemistry,
Pohang University of Science and Technology (POSTECH)
Pohang 37673 (Republic of Korea)
E-mail: ytchang@postech.ac.kr
[+] These authors contributed equally to this work.
Supporting information and the ORCID identification number(s) for the author(s) of this article can be found under: https://doi.org/10.1002/anie.201902766.

  

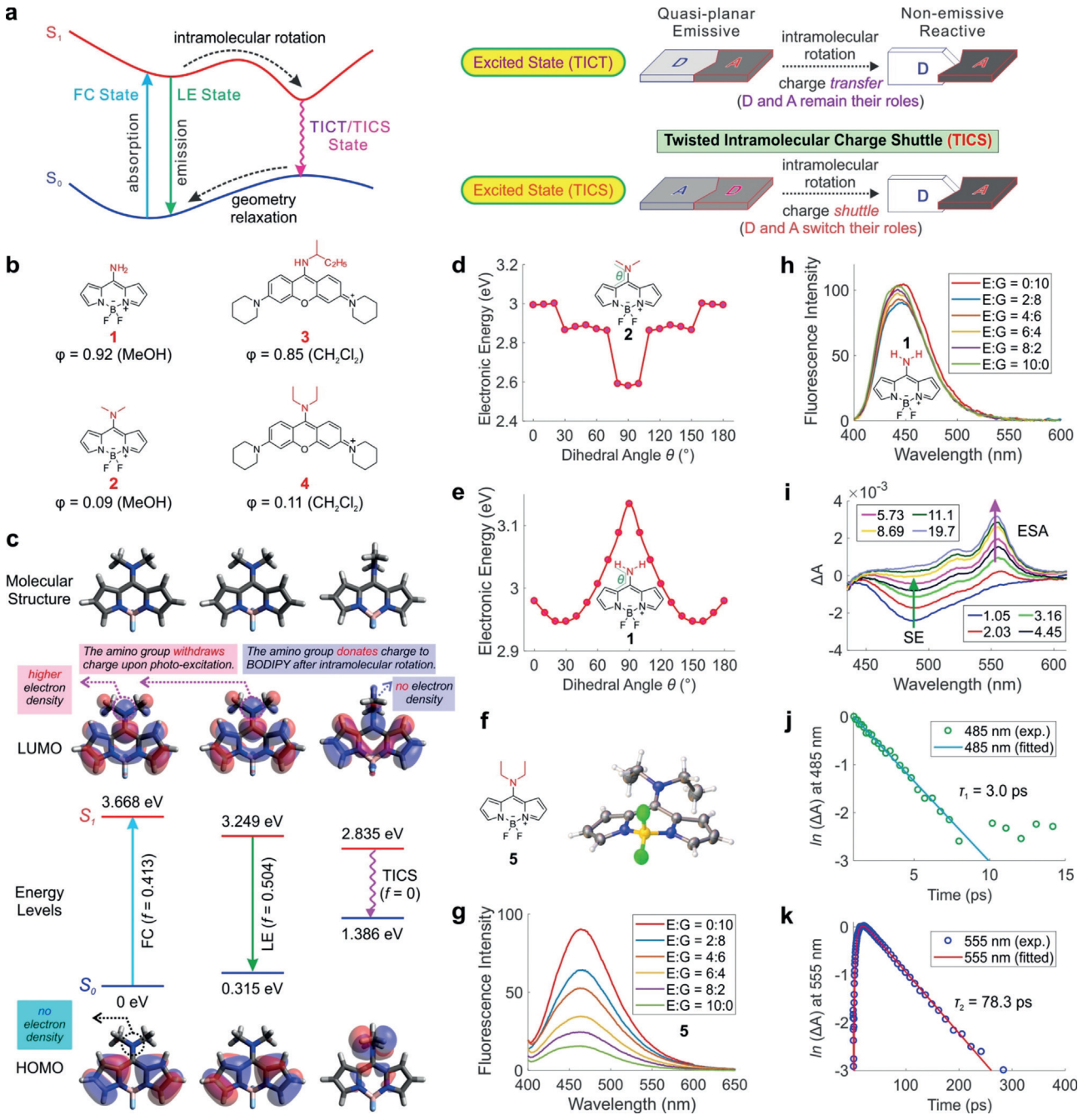


***Figure 1.*** a) Schematic illustration of the twisted intramolecular charge transfer/shuttle (TICT/TICS) mechanisms; "D" and "A" denote electron-donating and electron-accepting moieties, respectively. b) Representative TICS compounds and their quantum yields ($\varphi$). c) Optimized molecular structures, LUMO, HOMO, and relative energy levels of the ground ($S_0$) and excited ($S_1$) states during light absorption (FC, upward arrows), emission (LE, downward arrows), and the TICS state of **2** in ethanol. The energy level of **2** was computed using the linear solvation method. Calculated potential energy surfaces of d) **2** and e) **1** in the $S_1$ state in ethanol. f) Molecular structure and crystallographic asymmetric unit of **5** at room temperature with anisotropic displacement ellipsoids drawn at the 50% probability level. Fluorescence intensity changes of g) **5** and h) **1**, as a function of viscosity in the mixture of ethylene glycol (E) and glycerol (G). [**1**] = 10 μM; [**5**] = 10 μM; excitation wavelength: 380 nm. i) Transient absorption spectra of **5** in chloroform. Decay dynamics of the transient absorption spectra of **5** at j) 485 nm and k) 555 nm.

9% for **2** in methanol), as the *meso*-substituent changed from an amino group to a dimethylamino group (Figure 1b). To understand if a correlation between the amino groups and the quantum yields exists, we conducted data searches for similar compounds in chemical databases (Supporting Information, Table S1). The searches returned results with many BODIPY derivatives showing the same pattern, that is, attaching a dialkylated amino group at the *meso*-position led to substantially lower quantum yields (especially in polar solvents). Interestingly, further searches showed that this relationship holds true in rhodamine dyes (Supporting Information, Table S2), such as in compounds **3** ($\varphi$ = 85%)

and **4** ($\varphi = 11\,\%$ in $CH_2Cl_2$; Figure 1b). This trend led us to suspect that the low quantum yields in **2** and **4** were due to N–C bond rotations of the dialkylated amino groups, as in the TICT mechanism.

Next, we employed quantum chemical calculations to understand the molecular origins of the low quantum yields in **2** (Figure 1c and Supporting Information, Figures S1–S10). It is noted that the dimethylamino group at the *meso*-position of **2** was partially positively charged (+0.36e) in the ground state (Supporting Information, Figure S5) and acted as an EWG in the Franck–Condon (FC) state during light absorption. For example, upon photoexcitation, the electron density of the dimethylamino group greatly increases as substantial charge flows towards the *meso*-position of BODIPY (Figure 1c). In the excited state, compound **2** exhibited two stable conformations, and the most stable conformation was exemplified by an approximately 90° rotation between the dimethylamino group and the fluorophore scaffold. Moreover, the dimethylamino group remains as an EWG in the local excited (LE) state, similar to that in the FC state (Supporting Information, Figures S6 and S7). However, after the approximately 90° rotation, the dimethylamino group switched roles to become electron-donating (Supporting Information, Figure S8). Consequently, the electron density of the dimethylamino group was substantially reduced in the excited state as charge flowed back to the BODIPY scaffold (Figures 1c). In other words, the approximately 90° rotation in **2** is accompanied by a charge shuttle process, as the dimethylamino group switches roles from an EWG to an EDG. We term this a twisted intramolecular charge shuttle (TICS).

It is worth highlighting that the charge-shuttle process clearly differentiates **2** from the charge transfer in the TICT mechanism. During TICT formation, a fluorophore (such as coumarin 152; Supporting Information, Figure S11) also exhibits two stable conformations in the excited state, and the TICT state is characterized by an intramolecular rotation of approximately 90° between the fluorophore scaffold and the amino group. However, the amino group remains as an EDG both before and after the molecular rotations. In other words, the intramolecular rotations in TICT compounds enhance charge transfer but do not induce charge shuttling (Supporting Information, Figure S11). Moreover, TICT compounds display a positive solvatochromism, as charge transfer is enhanced in the excited state. In contrast, TICS compounds often exhibit a negative solvatochromism in UV/Vis absorption spectra, as the amino group withdraws charge, leading to a smaller dipole moment upon photo-excitation (Supporting Information, Tables S3 and S4, Figures S11, and S25–S29).

To gain more insights into the TICS mechanism, we calculated the potential energy surface (PES) of **2** in the first excited singlet state ($S_1$) as a function of amino group rotations (Figure 1d). This PES exhibited two stable conformations, corroborating our previous results. Notably, the TICS conformation is the global minima and the oscillator strength of the TICS conformation is almost zero, indicating that TICS is a dark state. The low quantum yield of **2** was thus ascribed to the formation of the TICS state. In contrast, PES calculations on **1** showed no other minima, i.e., apart from the LE state in the $S_1$ (Figure 1e), and the quantum yield of **1** is high in the absence of TICS.

To experimentally validate the TICS hypothesis in BODIPY dyes, we next synthesized and characterized two BODIPY derivatives, including **1** and **5** (Figure 1b,f). BODIPY **5** (a close analogue of **2**) exhibited low quantum yields (Supporting Information, Table S3). The molecular structure of **5** derived from its crystal structure (Figure 1f) agrees with our DFT calculations (Supporting Information, Tables S7 and S8). Moreover, as we increased solvent viscosity by introducing more glycerol in the ethylene glycol/glycerol mixtures, we noticed a considerable enhancement of fluorescence intensities by up to approximately 6 times in **5** (Figures 1g). These observations indicated that the low quantum yields of **5** were related to molecular rotations. In contrast, BODIPY **1** exhibited high quantum yields (Supporting Information, Table S4) and their emission intensities were not sensitive to solvent viscosities (Figure 1h). These results again corroborate our theoretical calculations.

We performed transient absorption spectroscopy measurements on **5** (Figure 1i and Supporting Information, Figures S38–S41). After photo-excitation, the experimental data revealed the co-existence of two excited states. The first excited state produced a stimulated emission band at approximately 480 nm, with a short decay lifetime of 3.0 ps (Figure 1j). We assigned this band to the LE state. The second excited state showed an excited state absorption band with a peak and a shoulder at 555 nm and 521 nm, respectively, and a much longer decay lifetime of 78.3 ps (Figure 1k). Note that in the TICS state, a negatively charged BODIPY radical will form upon the complete charge transfer from the amino group to the BODIPY scaffold. It was reported that this BODIPY radical has a transient absorption spectrum at approximately 550–580 nm (Supporting Information, Figure S42).[13] This is in good agreement with our observation. We thus attributed the second excited state to the TICS state. The transition rate from the LE to the TICS states was estimated to be $3.3 \times 10^{11}\ s^{-1}$.

Encouraged by the consistency between theoretical and experimental results, we next explored if the TICS model was also applicable to oxygen–rhodamines (Figure 2a and Supporting Information, S12–S14). Our calculations showed that dialkylated amino group substituted rhodamine **6** exhibited two stable conformations in the $S_1$ state, and the approximately 90° twisted conformation was the global minimum (Figure 2b). Moreover, **6** clearly exhibited the charge shuttle character: the amino group at the *meso*-position served as an EWG in the FC and LE states but switched to an EDG in the TICS state upon photoexcitation. Our calculations also showed that the primary amino substituted rhodamine **7** is not prone to TICS formation, as the twisted state is unstable in the PES of **7** (Figure 2c).

We next synthesized **6** and **7** and measured their spectral properties (Supporting Information, Tables S5 and S6 and Figures S30–S33). As predicated by our theoretical calculations, the quantum yield of **6** was very low due to substantial TICS formation, while **7** emitted bright fluorescence. These results also suggest that the TICS mechanism was not limited to BODIPY dyes but could exist in other dye families.

  

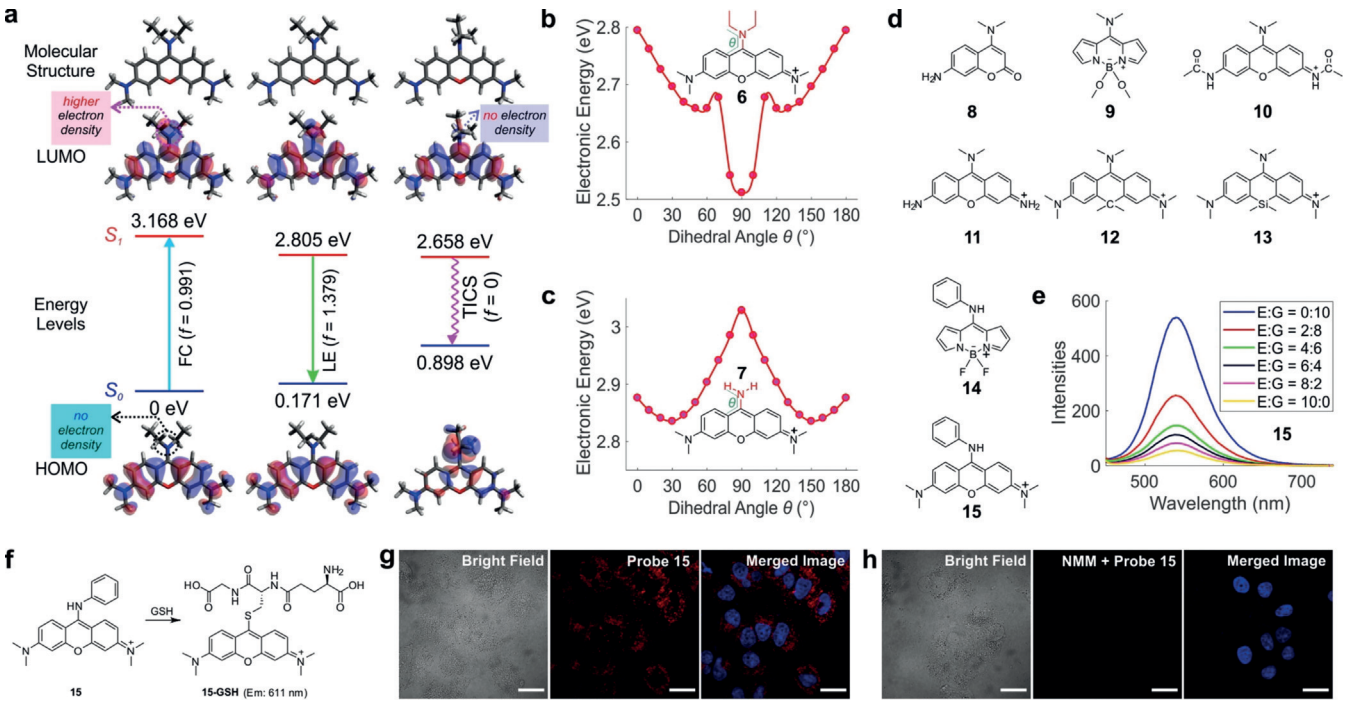


***Figure 2.*** a) Optimized molecular structures, LUMO, HOMO, and relative energy levels of the ground ($S_0$) and excited ($S_1$) states during light absorption (FC, upward arrows), emission (LE, downward arrows), and the TICS state of **6** in ethanol; HOMO was obtained with corrections using the state-specific solvation. Calculated potential energy surfaces of b) **6** and c) **7** in the $S_1$ state in ethanol. d) In-silico-designed TICS compounds. e) Viscosity dependence of emission intensities of **15** ([**15**] = 10 μM) in ethylene glycol (E) and glycerol (G) mixtures. f) Reaction mechanism of **15** and GSH. g and h) Confocal microscope images of HeLa cells stained with **15** and Hoechst 33342 for 120 min ([**15**] = 5 μM; [Hoechst 33342] = 3 μM. In (h) cells were pre-treated with 1 mM NMM for 20 min to remove GSH, followed by dye staining for 120 min. Blue channel: excitation wavelength = 405 nm; emission filter band-path 420–470 nm; red channel: excitation wavelength = 543 nm; emission filter band-path 570–620 nm. Scale bar = 20 μm.

As such, we computationally explored if TICS was applicable to various families of fluorophores. Theoretical calculations showed that TICS was energetically favourable in coumarin **8**, alkoxy BODIPY **9**, oxygen–rhodamine **10** and **11**, carbon–rhodamine **12**, and silicon–rhodamine **13** (Figure 2d and Supporting Information, Figures S15–S20). We also found that in TICS compounds, the amino group is not limited to dialkylated amino groups, but can be extended to aniline groups as well, such as in BODIPY **14** and rhodamine **15** (Supporting Information, Figures S21 and S22). Overall, these results demonstrate that TICS represents a general charge transfer and separation process, governing many different types of fluorophores.

Among these predicted TICS compounds, we synthesized **15**. Indeed, as the solvent viscosity increased, the emission intensities of **15** were greatly enhanced (Figure 2e). These results confirm the rotational nature of the TICS compound **15**.

Finally, significant rotations of the dialkylated amino moieties and the associated fluorescence quenching in the TICS state can be employed in many practical applications.[14] Inspired by the pioneering work of de Silva et al.,[5b] we are interested in applying TICS compounds as fluorescent probes. Since the shuttle mechanism involves rotations of molecules, they are good candidates for quantifying solvent viscosities (such as with **5** and **15**; Figures 1g and 2e). Since TICS compounds possess low polarity, they could be insensitive to solvent polarity, making them dedicated viscosity probes.

We also expected that replacement/removal of the amino group at the *meso*-position could eliminate TICS and enhance emission intensities. Indeed, the reaction between **15** and glutathione (GSH) removed the *meso*-aniline group and turned on bright red emissions that peaked at 611 nm (Figure 2f). Furthermore, in vitro experiments showed that **15** was highly selective for GSH (Supporting Information, Figures S34–S37). We next proceeded to perform live-cell experiments. Upon staining HeLa cells with 5 μM probe **15** and 3 μM Hoechst 33342 (a nucleus stain) for 2 h, bright emissions from both the red channel and the blue channel were observed (due to the presence of GSH and nucleus, respectively; Figure 2g). In contrast, by pre-treating cells with 1 mM *N*-methylmaleimide (NMM) to remove GSH, we observed no red emission in this control group, but only blue emissions from the nucleus (Figure 2h). These experiments demonstrated that TICS compound **15** is a promising GSH probe for both in vitro and in vivo experiments. Interestingly, we also noted many existing NO and phosgene fluorescent probes belong to the TICS family (Supporting Information, Figures S23 and S24).

In conclusion, we have discovered a new charge transfer and separation process, namely twisted intramolecular charge shuttle (TICS), through chemical database searches, quantum chemical rationalization, and experimental validation. In

  

TICS compounds, the dialkylated amino (or aniline) group acts as an electron-withdrawing group upon light absorption and then becomes an electron-donating group after the approximately 90° intramolecular rotation. This unique role switching and charge shuttling process differentiates TICS from the TICT mechanism. We also demonstrated that TICS is applicable to a wide range of chemical families of fluorophores and can be employed to construct useful fluorescent probes. The discovery of the TICS mechanism provides an expansive view on charge-transfer and separation processes existing in nature and will inspire potential applications.

## Acknowledgements

W.C., R.L., and X.L. were supported by SUTD and the SUTD-MIT International Design Centre (IDC) [T1SRCI17126, IDD21700101, IDG31800104]. Q.Q., W.L., and Z.X. were supported by the NSFC (21878286, 21502189) and DICP (DMTO201603, TMSR201601). Y.S.T., D.G., and M.J.L. were supported by the NRF Singapore through SMART Centre's BioSyM IRG research program. Y.T.C. was supported by the Institute for Basic Science (IBS) [IBS-R007-A1]. The authors would like to acknowledge the use of the computing service of SUTD-MIT IDC and NSCC.

## Conflict of interest

The authors declare no conflict of interest.

**Keywords:** charge transfer and separation · fluorescent probes · fluorophore · biosensors · donor–acceptor systems

**How to cite:** *Angew. Chem. Int. Ed.* **2019**, *58*, 7073 – 7077
*Angew. Chem.* **2019**, *131*, 7147 – 7151

[1] a) Z. R. Grabowski, K. Rotkiewicz, W. Rettig, *Chem. Rev.* **2003**, *103*, 3899 – 4032; b) W. Rettig, *Angew. Chem. Int. Ed. Engl.* **1986**, *25*, 971 – 988; *Angew. Chem.* **1986**, *98*, 969 – 986.

[2] a) G. D. Scholes, G. R. Fleming, A. Olaya-Castro, R. Van Grondelle, *Nat. Chem.* **2011**, *3*, 763; b) M. S. Eberhart, L. M. R. Bowers, B. Shan, L. Troian-Gautier, M. K. Brennaman, J. M. Papanikolas, T. J. Meyer, *J. Am. Chem. Soc.* **2018**, *140*, 9823 – 9826.

[3] a) J. Liu, S. Chen, D. Qian, B. Gautam, G. Yang, J. Zhao, J. Bergqvist, F. Zhang, W. Ma, H. Ade, *Nat. Energy* **2016**, *1*, 16089; b) Z. Zheng, O. M. Awartani, B. Gautam, D. Liu, Y. Qin, W. Li, A. Bataller, K. Gundogdu, H. Ade, J. Hou, *Adv. Mater.* **2017**, *29*, 1604241.

[4] a) D. M. Schultz, T. P. Yoon, *Science* **2014**, *343*, 1239176; b) Q. Wang, T. Hisatomi, Q. Jia, H. Tokudome, M. Zhong, C. Wang, Z. Pan, T. Takata, M. Nakabayashi, N. Shibata, *Nat. Mater.* **2016**, *15*, 611.

[5] a) Z. Guo, S. Park, J. Yoon, I. Shin, *Chem. Soc. Rev.* **2014**, *43*, 16 – 29; b) A. P. De Silva, H. N. Gunaratne, T. Gunnlaugsson, A. J. Huxley, C. P. McCoy, J. T. Rademacher, T. E. Rice, *Chem. Rev.* **1997**, *97*, 1515 – 1566.

[6] a) S. Wang, X. Yan, Z. Cheng, H. Zhang, Y. Liu, Y. Wang, *Angew. Chem. Int. Ed.* **2015**, *54*, 13068 – 13072; *Angew. Chem.* **2015**, *127*, 13260 – 13264; b) S. Sasaki, G. P. Drummen, G.-i. Konishi, *J. Mater. Chem. C* **2016**, *4*, 2731 – 2743; c) W. G. Santos, D. S. Budkina, V. M. Deflon, A. N. Tarnovsky, D. R. Cardoso, M. D. Forbes, *J. Am. Chem. Soc.* **2017**, *139*, 7681 – 7684; d) Q. Zhang, H. Kuwabara, W. J. Potscavage, Jr., S. Huang, Y. Hatae, T. Shibata, C. Adachi, *J. Am. Chem. Soc.* **2014**, *136*, 18070 – 18081.

[7] a) X. Liu, J. M. Cole, P. G. Waddell, T.-C. Lin, J. Radia, A. Zeidler, *J. Phys. Chem. A* **2012**, *116*, 727 – 737; b) A. Romieu, G. Dejouy, I. E. Valverde, *Tetrahedron Lett.* **2018**, *59*, 4574 – 4581.

[8] K. Rotkiewicz, K. Grellmann, Z. Grabowski, *Chem. Phys. Lett.* **1973**, *19*, 315 – 318.

[9] R. Ghosh, *Phys. Chem. Chem. Phys.* **2018**, *20*, 6347 – 6353.

[10] a) J. B. Grimm, B. P. English, J. Chen, J. P. Slaughter, Z. Zhang, A. Revyakin, R. Patel, J. J. Macklin, D. Normanno, R. H. Singer, *Nat. Methods* **2015**, *12*, 244; b) X. Liu, Q. Qiao, W. Tian, W. Liu, J. Chen, M. J. Lang, Z. Xu, *J. Am. Chem. Soc.* **2016**, *138*, 6960 – 6963.

[11] T. Myochin, K. Hanaoka, S. Iwaki, T. Ueno, T. Komatsu, T. Terai, T. Nagano, Y. Urano, *J. Am. Chem. Soc.* **2015**, *137*, 4759 – 4765.

[12] M. A. Haidekker, T. P. Brady, D. Lichlyter, E. A. Theodorakis, *J. Am. Chem. Soc.* **2006**, *128*, 398 – 399.

[13] a) J. T. Buck, A. M. Boudreau, A. DeCarmine, R. W. Wilson, J. Hampsey, T. Mani, *Chem* **2019**, *5*, 138 – 155; b) M. A. Filatov, S. Karuthedath, P. M. Polestshuk, H. Savoie, K. J. Flanagan, C. Sy, E. Sitte, M. Telitchko, F. Laquai, R. W. Boyle, M. O. Senge, *J. Am. Chem. Soc.* **2017**, *139*, 6282 – 6285.

[14] D. Su, C. L. Teoh, L. Wang, X. Liu, Y.-T. Chang, *Chem. Soc. Rev.* **2017**, *46*, 4833 – 4844.

Manuscript received: March 4, 2019
Accepted manuscript online: March 27, 2019
Version of record online: April 12, 2019

  